Petroleum Science 20 (2023) 1513–1520

Contents lists available at ScienceDirect

Petroleum Science

journal homepage: www.keaipublishing.com/en/journals/petroleum-science

Original Paper

The application of Gaussian distribution deconvolution method to separate the overlapping signals in the 2D NMR map

Kou-Qi Liu [a, *], Zheng-Chen Zhang [a], Mehdi Ostadhassan [b, c]

[a] Institute of Energy, Peking University, Beijing, 100871, China
[b] Institute of Geosciences, Marine and Land Geomechanics and Geotectonics, Christian-Albrechts-Universität, Kiel, Germany
[c] Department of Geology, Ferdowsi University of Mashhad, Mashhad, Iran

ARTICLE INFO

Article history:
Received 13 July 2022
Received in revised form
22 August 2022
Accepted 3 November 2022
Available online 8 November 2022

Edited by Teng Zhu and Jie Hao

Keywords:
2D NMR
Signal amplitude
Gaussian distribution
Shale formations

ABSTRACT

The 2D NMR (T_1-T_2) mapping technique, which can be used to separate different proton populations from various sources (hydroxyls, solid organic matter, free water, and free HC) has gained attention in petroleum industry. To separate proton contributions, a fixed straight line is commonly employed to separate different regions representing proton sources on the map. However, some of these regions (Region 1 and 2) might overlap which makes extracting the NMR signal amplitude from these regions inaccurate. In order to solve this issue, in this study, we applied the Gaussian distribution deconvolution method to separate the T_1 and T_2 relaxation distributions and then derived the signal amplitude of each region instead of following the common fixed line approach. Next, we employed this method to analyze several shale samples from the literature and compared the results following both methods to verify our methodology. Finally, samples from the Bakken Shale were studied to separate signals from Region 1 and Region 2 and correlated the results with geochemical properties that were obtained from programmed (Rock Eval) pyrolysis. Results demonstrated an improvement in their relation when our approach is employed compared to the fixed line technique to differentiate signal from overlapping regions. This means the Gaussian distribution deconvolution method can be used with confidence to provide us with more accurate petrophysical and geochemical understanding of complex formations.

1. Introduction

Nuclear magnetic resonance (NMR) has already become an important tool to characterize the properties of shale plays, such as the total porosity and saturation. In one dimensional low field (2 MHz) NMR by applying the Carr-Purcell-Meiboom-Gill (CPMG) pulse sequence, the total porosity, pore size distribution, and permeability can be derived based on the transverse relaxation time distribution (T_2) (Dunn et al., 2002). However, the T_2 measurement cannot be used for quantifying the saturations of different protons such as oil and water due to the overlapping signals of these components on the T_2 relaxation distribution (Krumm and Howard, 2019). The recent application of the 2D NMR (T_1-T_2) mapping technique which can separate the signals of different protons in the study of shale plays has gained attention of researchers to make it a common petrophysical method in petroleum industry (Tinni et al., 2014; Nicot et al., 2016; Fleury and Romero-Sarmiento, 2016; Kausik et al., 2016; Chen et al., 2019).

T_1 and T_2 are fundamentally different relaxation mechanisms occurring simultaneously and independently. T_1 relaxation measures the net magnetization of flipped or inverted protons in a thermodynamically unstable state, which is highly dependent on the strength of the magnetic fields while T_2 relaxation measures the net magnetization in the transverse plane (Krumm and Howard, 2019). Since the transverse relaxation is sensitive to more interactive terms than the longitudinal relaxation, and the T_1 relaxation time is always larger than the T_2 relaxation time (Callaghan, 1999). Based on this, researchers have divided the 2D NMR maps that is the T_1-T_2 relationship display into different regions representing different proton contributing population and then calculate the signal amplitude of each region. In this regard, Khatibi et al. (2019) found that the NMR signal amplitude in the organic matter region can be a representative of the geochemical properties. They explained that the T_1/T_2 ratio has the power law

* Corresponding author.
E-mail address: kouqi.liu@pku.edu.cn (K.-Q. Liu).

https://doi.org/10.1016/j.petsci.2022.11.006

correlation with the maturity and the signal amplitude of the organic matter region is linearly correlated with the S_2 parameter derived from the routine Rock-Eval analysis. Li et al. (2018, 2020) argued that the S_1 parameter from the Rock-Eval would increase if the signal amplitude of the free oil region increases. Although studies in this field are still limited, they show the 2D NMR mapping technique which can be a useful tool to estimate the geochemical properties of the shale samples if the signal amplitude of each region can be derived accurately.

Based on what was said above, the signal amplitude of each region is largely dependent on the separation of each region. However, researchers have used different criteria to separate these regions on the map. Krumm and Howard (2019) explained that the region representing the organic matter on the 2D NMR map should be in the range of $10 < T_1 < 100$ ms and $T_1/T_2 > 10$. Li et al. (2020) studied the shale samples from the Jiyang Depression of China and found that the region of the organic matter should be $10 < T_1 < 1000$ ms and $T_1/T_2 > 100$. Khatibi et al. (2019) in the study of the Bakken Shale samples with different maturities showed that the line dividing the organic matter and the hydroxyls regions could vary from one sample to another. Fleury and Romero-Sarmiento (2016) studied extracted organic matter from the mineral matrix and concluded that the organic matter region will change as the maturity progresses. In their study, if the organic matter is immature, the region should be above the $T_1/T_2 = 50$ line, while for the organic matter in the gas window, the region will shift above the $T_1/T_2 = 180$ line. Furthermore, chemical structure of the organic matter based on its maturity or kerogen type, could impact the positioning of the organic matter region in the 2D NMR map. All of these above findings points to the fact that using the constant dividing line (such as the $T_1 = 10$ ms or the $T_1/T_2 > 10$) to separate different regions cannot be accurate. For example, Li et al. (2020) applied the line $T_1/T_2 = 100$ to separate the organic matter and hydroxyls regions while these two regions showed a very strong overlap. As a result, if regions exhibit a sharp boundary in the 2D NMR map, we can easily extract the signal amplitude from them otherwise the calculated amplitude cannot be trusted. A closer look at the maps from the studies cited here shows that in many of them the region representing the organic matter overlaps with the hydroxyl group (Liu et al., 2019; Li et al., 2020). This usually happens when the organic matter has flexible functional groups such as long aliphatic chains, the protons of the hydrogen in these parts which is mobile could cause short T_1 relaxation, overlapping with the hydroxyl signals (Song et al., 2008). Under these circumstances, using the constant dividing line which is still being used commonly to separate the overlapping area will introduce errors to our amplitude calculations. There is still a lack of consensus on the best method to separate these regions. Therefore, in this study, we proposed a new method based on the Gaussian distribution deconvolution to separate different regions of the 2D NMR map. Next, we applied this method to analyze published data in the literature and compared the results obtained from each method. Finally, our new approach was used to analyze shale samples from the Bakken for an improved correlation between the signals and the geochemical properties.

2. Method

Gaussian (normal) distribution is commonly used for 1D NMR data analysis. Atieh et al. (2013) used the Gaussian distribution to simulate the H^1-NMR signal of biofluids and found that the simulation results fit the experimental data. By applying the Gaussian distribution, Zhong et al. (2020) divided the T_2 relaxation time distribution into several zones, including clay bound water, capillary bound fluid, small pore fluid, and large pore fluid component spectrums. Based on the general properties of the spectral density functions at low and high frequencies for macromolecules in solution and using the principle of maximal entropy, Hsu et al. (2018) realized that the inverse Gaussian distribution function fits the NMR Spin-relaxation data. Jiang et al. (2019) studied the fluid components by using the T_1-T_2 NMR maps and regard the behavior of the fluid mixture can be assumed as a combination of Guassian distributions. Currently, there are many researchers that divided the 2D NMR map into several different regions (Khatibi et al., 2019; Liu et al., 2019; Li et al., 2020). For example, Liu et al. (2019) divided the 2D NMR map into four different regions as follows: Region 1, which is on the left bottom in the 2D NMR map (small T_2 and T_1/T_2 ratio), representing the hydroxyls part, Region 2 on the left top in the 2D map denoting the solid organic matter, Region 3 and Region 4 lie on the right bottom and top in the map, respectively, representing free water and free oil. In this study, we applied the Gaussian distribution method to separate the signal from the 2D NMR map into four different regions (the hydroxyls region on the left bottom, the solid organic matter region on the left top, the free water region on the right bottom and the free oil region on the right top) and derived the signal amplitude of each region, especially the hydroxyls region and the solid organic matter region. Two cases are considered in this study:

Case 1. The signal of Region 1 is overlapping with Region 3.

The 2D T_1-T_2 map of a real shale sample from the Bakken Formation is used to describe the procedures to separate the regions based on the Gaussian distribution. Fig. 1a shows that Region 4 has a clear boundary with the other three regions, which means the free oil region is always isolated from other regions (Khatibi et al., 2019; Liu et al., 2019; Li et al., 2020). However, Region 1 has some overlapping with Region 2 and Region 3. Here, we should first isolated Region 4 and extract its signal amplitude. Fig. 1a, c, e demonstrate the 2D NMR map, the T_2 relaxation distribution, and the T_1 relaxation distribution of the sample before Region 4 is isolated, respectively, while Fig. 1b, d, f is the 2D NMR map, the T_2 relaxation distribution, and the T_1 relaxation distribution of the sample after Region 4 is isolated, respectively. Fig. 1b displays that the T_2 time distribution of Region 3 differs from Region 1 and Region 2, while the T_1 time of Region 2 is different from the other two regions (Region 1 and Region 3). Then, the deconvolution method is applied for the signal analysis. Currently, there are several deconvolution techniques including the Wiener filtering, spectral extrapolation, minimum variance deconvolution, curve fitting method, wavelet method, the improved least-squares method, and the maximum correlated kurtosis method (Sin and Chen, 1992; Riad, 1986; Doyle, 1997; Tkachenko et al., 2013; Miao et al., 2017). In this study, we applied the Gaussian distribution to deconvolve the T_1 and T_2 relaxation distributions, respectively (Ulm et al., 2007; Liu et al., 2017). We assumed that the total signal amplitude following eliminating signal from Region 4 (Fig. 1b) can be divided into three groups with sufficient contrast in T_1 or T_2 relaxation distributions ($J = 1, 2, 3$). The J_{th} group occupies a volume fraction f_J of the total signal amplitude. The theoretical probability density function (PDF) of the single phase, which is assumed to fit a normal distribution is defined as:

$$P_J(x_i, U_J, S_J) = \frac{2}{\sqrt{2\pi(S_J)^2}} \exp\left(\frac{(x_i - (U_J))^2}{2(S_J)^2}\right), \quad (1)$$

where U_J and S_J are the mean value and the standard deviation of distributions of the group $J = 1$ to 3. By minimizing the difference between the data from the model PDF and the experimental PDF, the unknowns $\{f_J, U_J, S_J, \}$ can be derived:

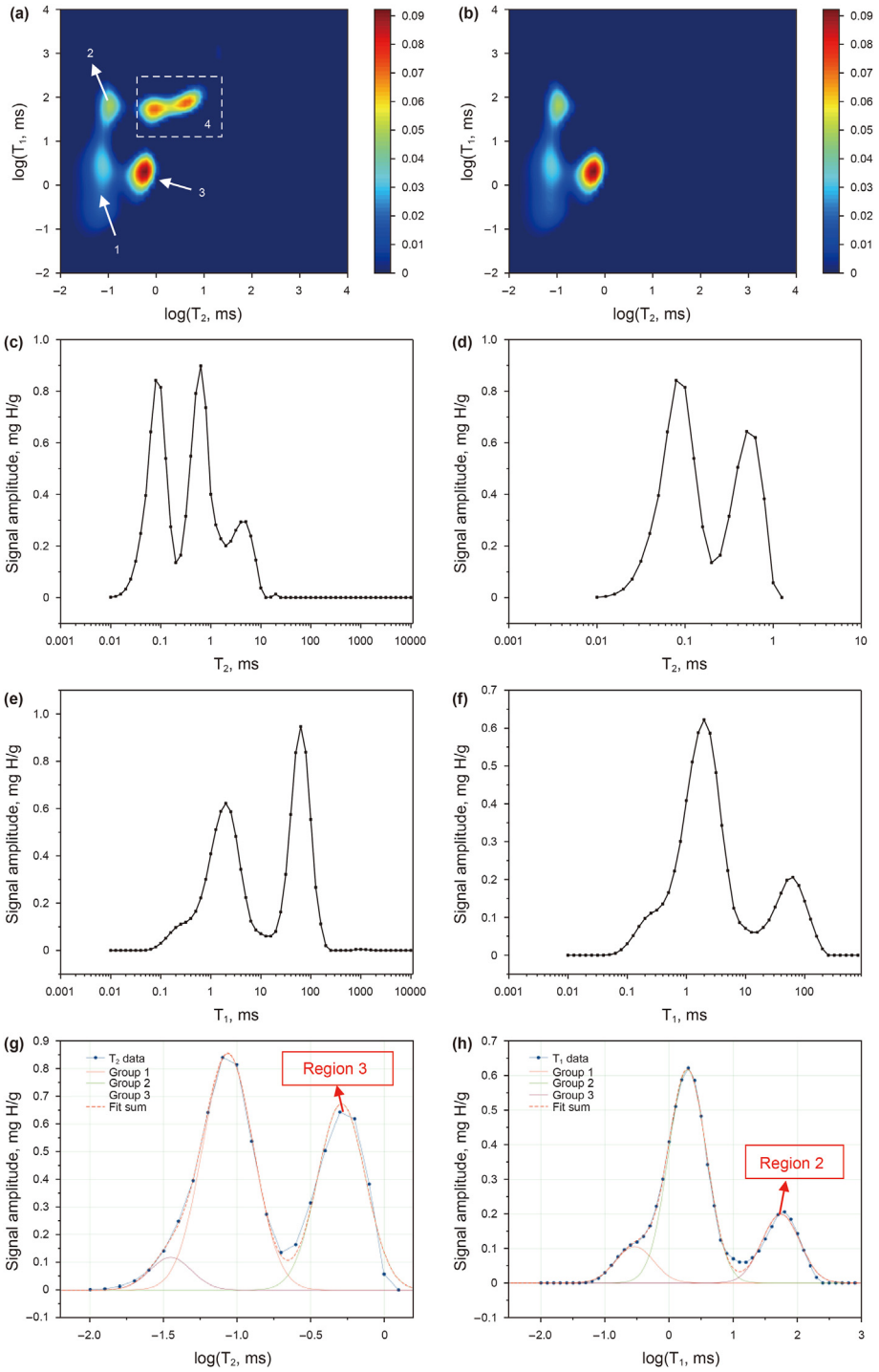

Fig. 1. The 2D NMR T_1-T_2 analysis of the shale sample (a, c, e shows the 2D NMR map, the T_2 relaxation distribution, and the T_1 relaxation distribution of the sample before removing Region 4, while b, d, f show the 2D NMR map, the T_2 relaxation distribution, and the T_1 relaxation distribution of the sample after removing Region 4; g and h show the Gaussian distribution deconvolution of T_2 and T_1 relaxation distribution after removing Region 4, respectively).

$$\min\left[\sum_{i=1}^{m}\sum_{J}^{N}\left(\sum_{J}^{n} f_J P_J\left(x_i, U_J, S_J\right) - P_x(x_i)\right)^2\right] \tag{2}$$

$$\sum_{J=1}^{n} f_J = 1 \tag{3}$$

$$U_J + S_J < U_{J+1} + S_{J+1} \tag{4}$$

In the above equation, P_x (x_i) is the measured value of the normalized frequency of the size x_i and m is the number of the

intervals (bins). Equation 6 is added to ensure different groups have sufficient contrast (Sorelli et al., 2008). Based on the Gaussian distribution deconvolution, we used the T_1 and T_2 relaxation distributions to obtain the signal amplitude of Region 2 and Region 3, respectively (Fig. 1g and h). Finally, the signal of Region 1 can be calculated, which is the difference between the total signal amplitude after the signal pertaining Region 4 is eliminated and the sum of the signal amplitude of Regions 2 and 3.

Case 2. The signal of Region 1 is not overlapping with Region 3.

One special case in 2D NMR relaxometry of shale samples would be when Region 3 and Region 4 all have clear boundaries with Region 1 and Region 2 (Fig. 2a). The example we studied below is from published data by Liu et al. (2019). The general workflow is similar to the previous case, when we first remove the signal from Region 4 as shown in Fig. 2b and then, the signal from Region 3 is extracted (Fig. 2c). The remaining signal after removal of Region 3 and 4 will be the sum of signal amplitude of Region 1 and 2. Since each of these regions have very different T_1 time distributions, the deconvolution of the T_1 relaxation distribution (after the removal of Region 3 and Region 4) can be used to obtain the signal amplitude of Region 1 and Region 2 (Fig. 2d).

Overall, the schematic of the procedure to obtain the signal amplitude of these four different regions based on the above two different examples can be found in Fig. 3.

3. Method verification and comparison

In this part, we will employ our proposed method to separate the signal amplitude of each region of the samples that have been published by Liu et al. (2019). In their study, they applied the $T_1 = 10$ ms as the fixed dividing line to separate Region 1 and Region 2 and derived the signal amplitude of each region. The comparison of the results which is shown in Fig. 4 explains that the signal amplitudes of Regions 3 and 4 from this study and what is obtained by Liu et al. (2019) are very close. However, there is a discrepancy based on the sample in the signal amplitudes of Regions 1 and 2 (e.g., Sample 8 vs. Sample 2). The potential reason could be that Region 1 and 2 in Sample 2 compared to Sample 8 have larger overlapping areas (Fig. 5). We further correlated the absolute signal amplitude differences of Region 2 of all samples which is defined as the signal amplitude derived from this study minus the signal amplitude derived from Liu et al. (2019), with the thermal maturity

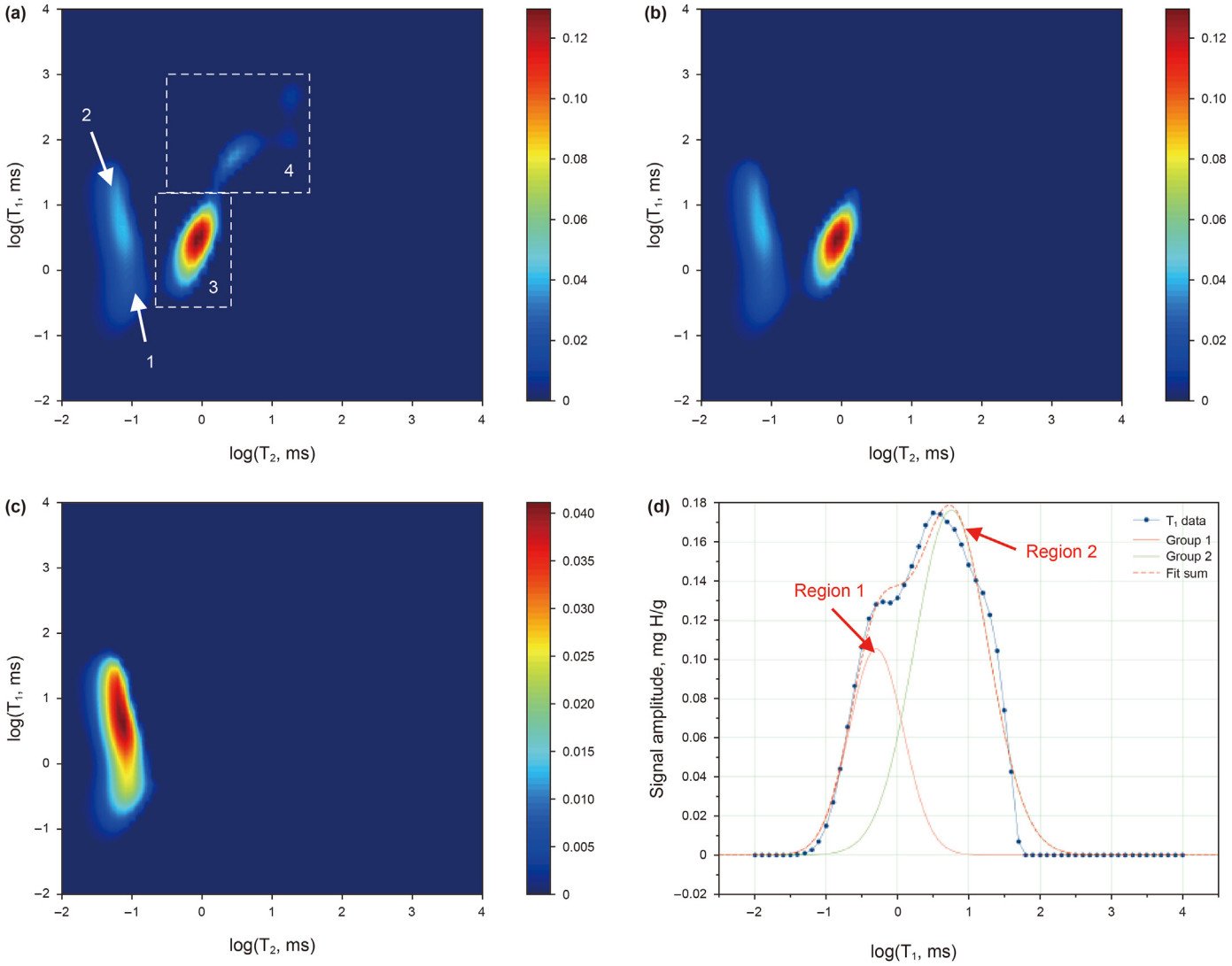

Fig. 2. The 2D NMR map analysis of shale sample (a shows the 2D NMR map of all the regions; b is the 2D NMR map after removing Region 4; c is the 2D NMR map after removing 3 and 4; d is the data deconvolution of T_1 relaxation distribution of c).

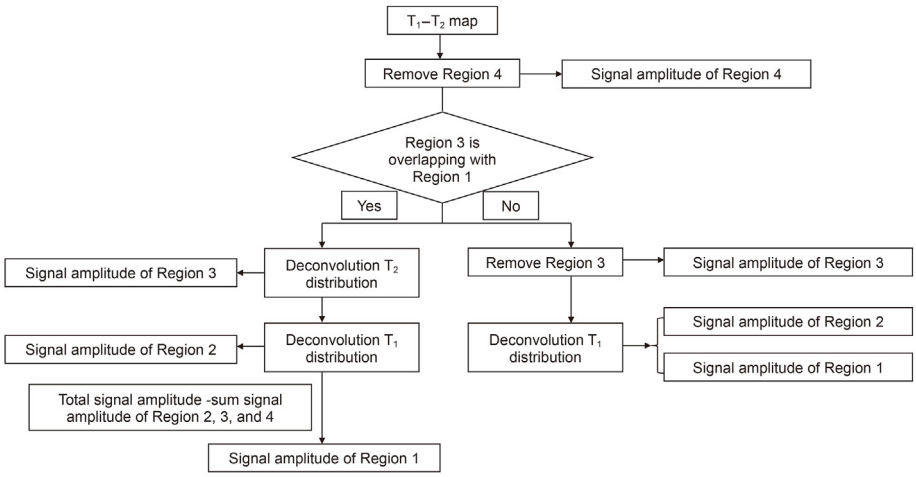

Fig. 3. Schematic of calculating the signal amplitude of each region from the 2D NMR map.

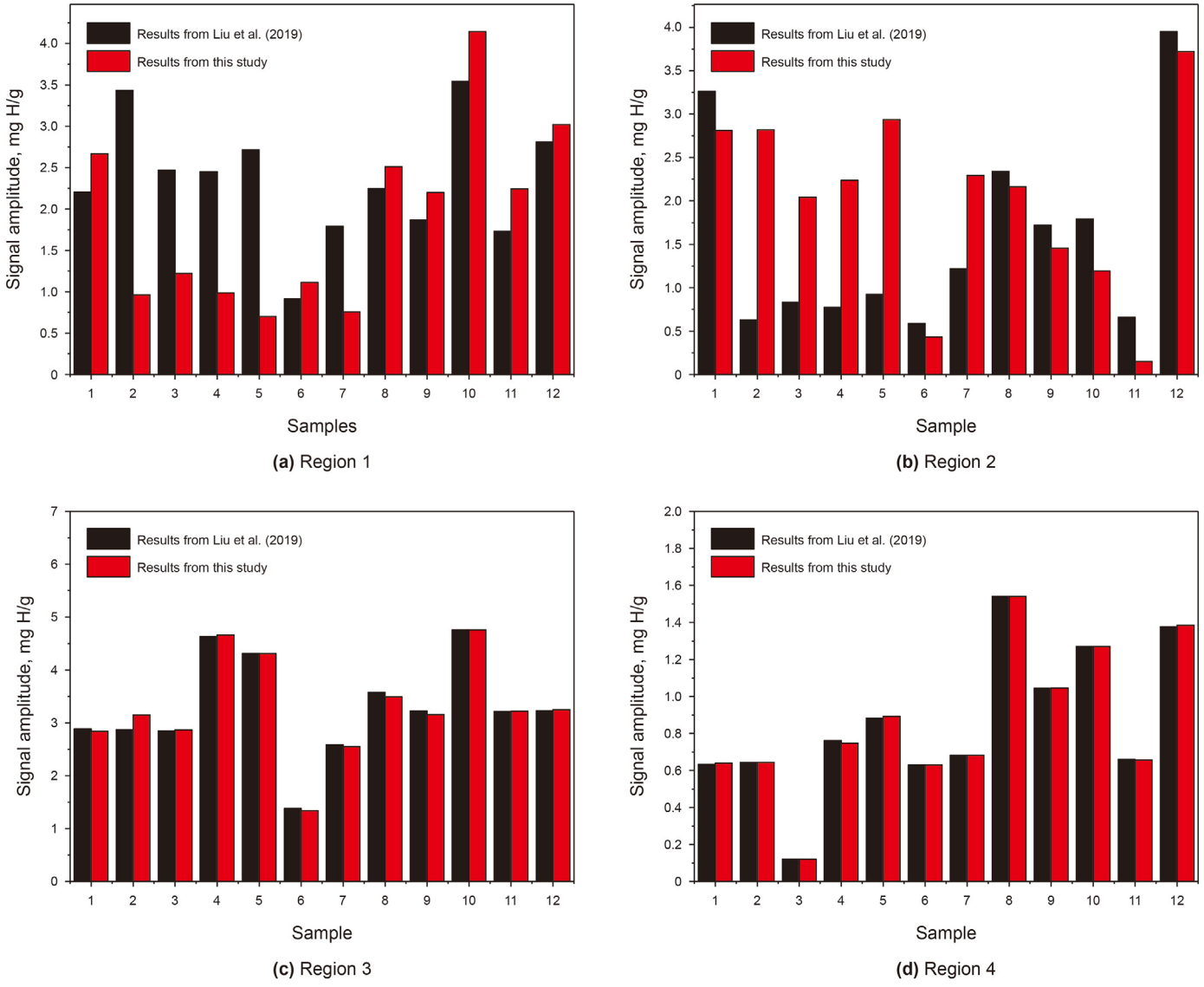

Fig. 4. Comparisons of the signal amplitude of each region from this study and the results from Liu et al. (2019).

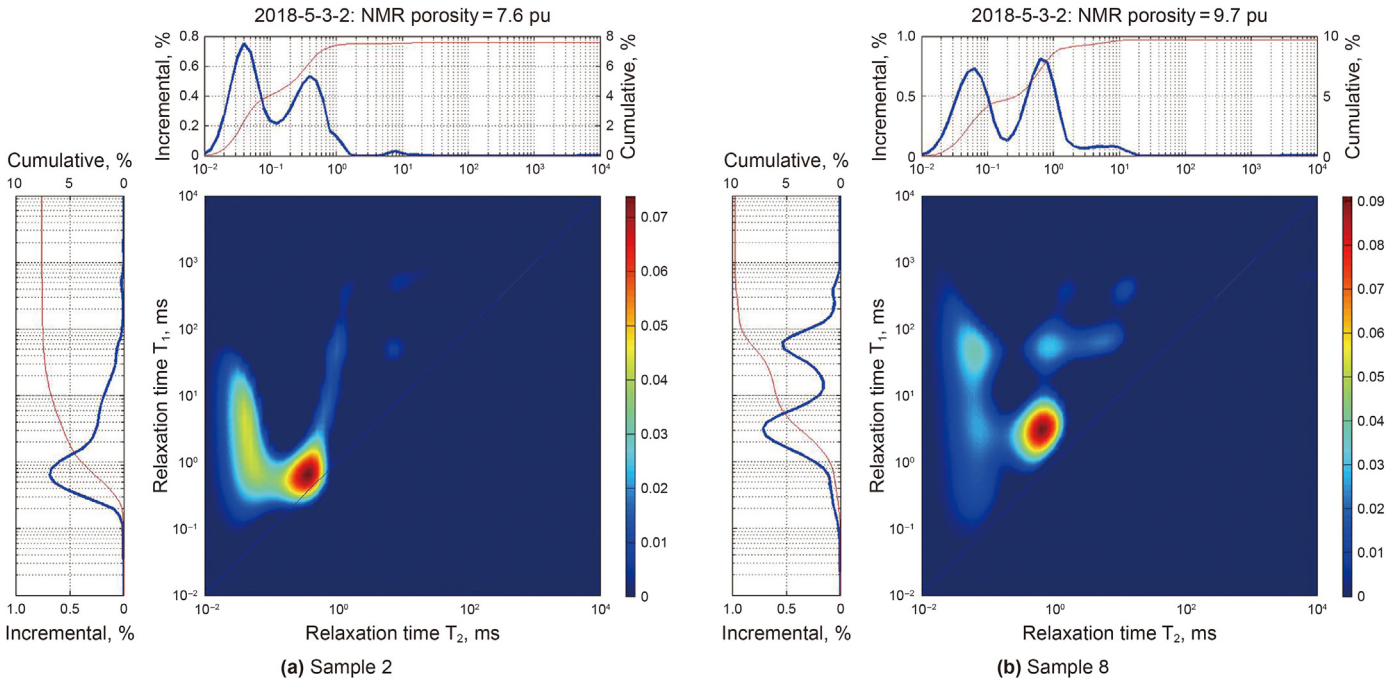

Fig. 5. The 2D NMR maps of Sample 2 (a) and Sample 8 (b) (Liu et al., 2019).

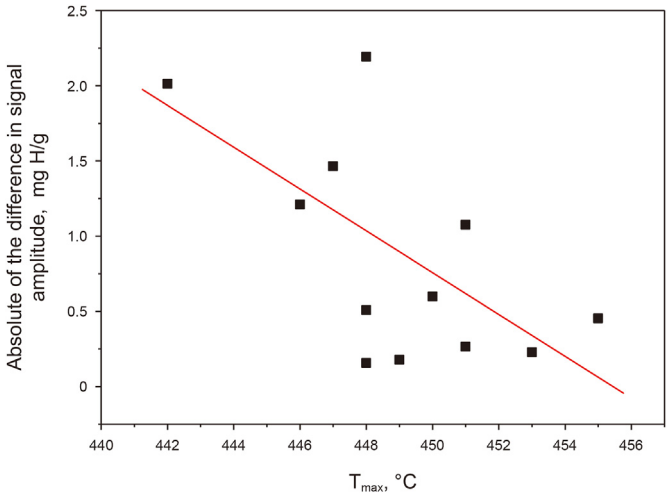

Fig. 6. Correlation between the signal difference of Region 2 and T_{max}.

indicator, T_{max}. Fig. 6 depicts that as the maturity of the shale samples increases (T_{max} increases), the absolute value of the difference in the signal amplitude of Region 2 regardless of the method that is being used shows a decreasing trend. This is due to the fact that, the organic matter becomes more compacted due to the clusters that are formed by the aromatic rings with increasing maturity, which causes an increase in the density of the organic matter macromolecule, causing a decrease in the mobility of the protons in the kerogen. This will result in an increase in the T_1 relaxation time of the organic matter to become longer (Lee et al., 2020). Thus, the overlapping of the signal from the organic matter and the hydroxyl group will decrease with the progression of thermal maturity.

Overall, if the signal in the 2D NMR map of each region shows clear boundaries (for high mature shale samples), then different regions can be separated to simply attain signal amplitude of each region. However, if regions have some overlapping (for relatively lower thermally mature samples), using the strict constant dividing line to separate the regions and obtain the signal amplitude of different regions will not provide us accurate output. This means the larger the overlapping areas will lead to a larger error when the constant dividing line approach is employed. Therefore, applying the Gaussian distribution to analyze the overlapping zones of 2D NMR T_1-T_2 data could lead to better results of the signal amplitude of each region.

4. Method application in Bakken shale formation

Several researchers have applied the constant dividing line to derive the amplitude of different regions and then correlate the amplitude of these regions with geochemical parameters that are derived from Rock-Eval pyrolysis (Li et al., 2020; Khatibi et al., 2019; Liu et al., 2019). However, from our study, if the samples are in the lower maturity stages, the amplitude that is calculated from the fixed dividing lines could have a lower correlation compared to our method since the signal amplitude that is obtained is not reliable. In order to find the correlations between the signals of the different regions and the geochemical properties, we applied the deconvolution method proposed here to study the Bakken shale samples and investigate how the signal amplitude from our method will correlated with geochemical properties compared to the common fixed line approach. We analyzed 2D NMR of 24 Bakken shale samples and calculated the signal of each region of these samples. Fig. 7 shows that the mean value of the Region 2 ($\log(T_1)$) increases with the T_{max}, which could be due to the slower mobility of the protons of the organic matter as the structure becomes more compact (Lee et al., 2020). Fig. 8 exhibits that the intensity of Region 1 is negatively correlated with T_{max}. The signal of Region 1 is mainly attributing to the hydroxyl group, i.e., the OH which is related to the clay minerals (the structural water or the absorbed water) (Li et al., 2020; Khatibi et al., 2019). As the thermal maturity of the samples increases, either the adsorbed water or the structural water

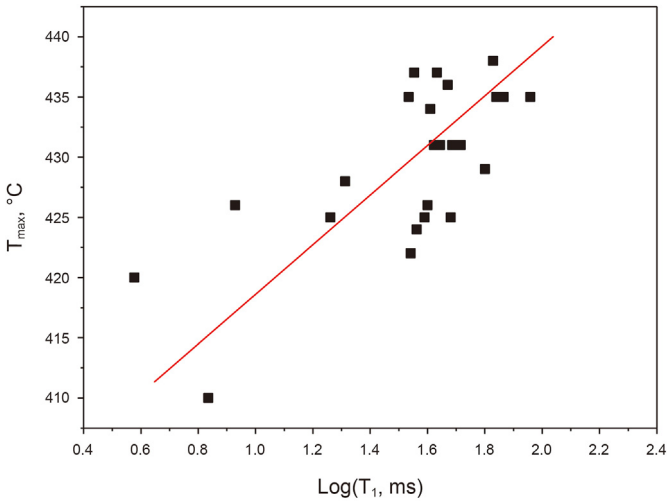

Fig. 7. Correlation between the T_{max} and log(T_1).

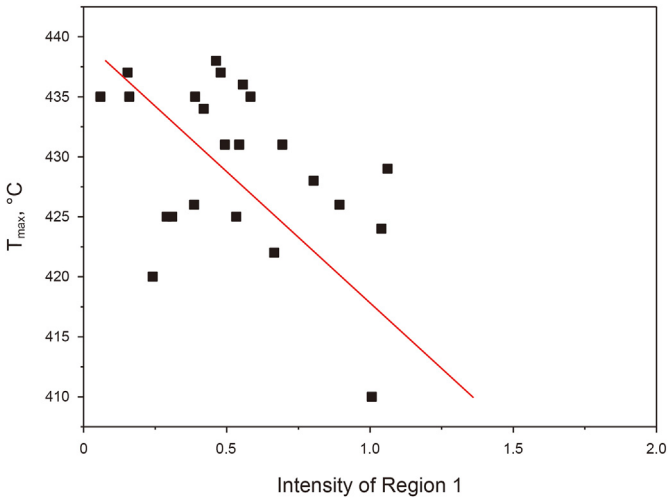

Fig. 8. Correlation between the T_{max} and intensity of the Region 1.

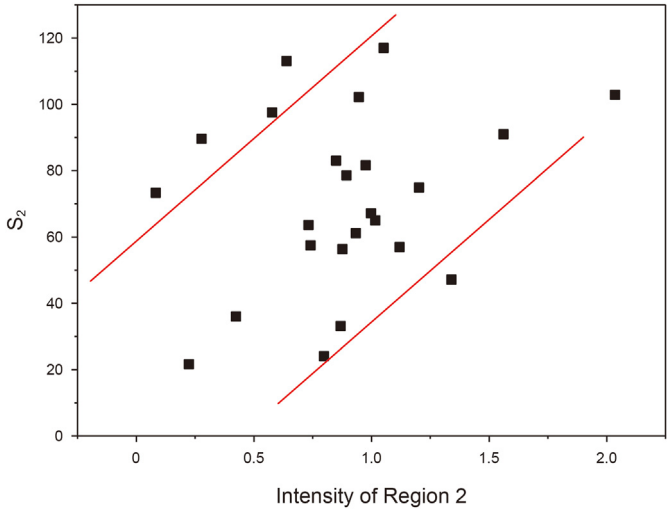

Fig. 9. Correlation between S_2 and intensity of the Region 2.

quantity reduces due to either the clay mineral conversion or the water desorption (Liu et al., 2021). In addition, S_2 which indicates the potential of the source rock to generate hydrocarbons upon heating shows a positive correlation with the intensity of Region 2, demonstrating that the amplitude of Region 2 can be used to indicate the hydrocarbon potential generation of source rocks (see Fig. 9).

5. Conclusions

In this study, we proposed a method to derive the signal amplitude from the overlapping regions based on the Gaussian distribution deconvolution on the T_1 and T_2 relaxation distributions. Then, we used the method to study the 2D NMR shale samples from the literature and compared the results with his study. The results showed that due to the overlapping of Region 1 (hydroxyls part) and Region 2 (solid organic matter), the signal amplitude of these two regions in this study using the Gaussian distribution deconvolution are different compared to the fixed line approach to divide the regions. The larger the overlapping (for low mature shale samples), the larger the difference of the signal amplitude of Region 2 would become. Finally, we applied the deconvolution method to study the Bakken shale samples and argued that the mean value of log(T_1) and the amplitude of Region 1 correlate well with the thermal maturity index (T_{max}), while the amplitude of Region 2 can be used to estimate the hydrocarbon generation potential of source rocks that is obtained from programmed pyrolysis. Generally speaking, this study provided a better approach to separate the signal amplitude of the regions with overlapping of NMR data for more accurate analysis of shale plays.

Acknowledgement

The authors appreciate the support from the National Natural Science Foundation of China (42090020,42090025,42272150) and the Sinopec Science and Technology Department (No. P20049-1).

References

Atieh, Z., Suhre, K., Bensmail, H., 2013. MetFlexo: an automated simulation of realistic H^1-NMR spectra. Procedia Comput. Sci. 18, 1382–1391. https://doi.org/10.1016/j.procs.2013.05.305.

Callaghan, P.T., 1999. Rheo-NMR: nuclear magnetic resonance and the rheology of complex fluids. Rep. Prog. Phys. 62 (4), 599.

Chen, Z., Singer, P.M., Wang, X., Vinegar, H.J., Nguyen, S.V., Hirasaki, G.J., 2019. NMR evaluation of light-hydrocarbon composition, pore size, and tortuosity in organic-rich chalks. Petrophysics 60, 771–797. https://doi.org/10.30632/PJV60N6-2019a5, 06.

Doyle, J.F., 1997. A wavelet deconvolution method for impact force identification. Exp. Mech. 37 (4), 403–408. https://doi.org/10.1007/BF02317305.

Dunn, K.J., Bergman, D.J., LaTorraca, G.A., 2002. Nuclear Magnetic Resonance: Petrophysical and Logging Applications. Elsevier.

Fleury, M., Romero-Sarmiento, M., 2016. Characterization of shales using T_1–T_2 NMR maps. J. Petrol. Sci. Eng. 137, 55–62. https://doi.org/10.1016/j.petrol.2015.11.006.

Hsu, A., Ferrage, F., Palmer III, A.G., 2018. Analysis of NMR spin-relaxation data using an inverse Gaussian distribution function. Biophys. J. 115 (12), 2301–2309. https://doi.org/10.1016/j.bpj.2018.10.030.

Jiang, H., Daigle, H., Tian, X., Pyrcz, M.J., Griffith, C., Zhang, B., 2019. A comparison of clustering algorithms applied to fluid characterization using NMR T_1-T_2 maps of shale. Comput. Geosci. 126, 52–61. https://doi.org/10.1016/j.cageo.2019.01.021.

Kausik, R., Fellah, K., Rylander, E., Singer, P.M., Lewis, R.E., Sinclair, S.M., 2016. NMR relaxometry in shale and implications for logging. Petrophysics 57, 339–350, 04.

Khatibi, S., Ostadhassan, M., Xie, Z.H., Gentzis, T., Bubach, B., Gan, Z., Carvajal-Ortiz, H., 2019. NMR relaxometry a new approach to detect geochemical properties of organic matter in tight shales. Fuel 235, 167–177. https://doi.org/10.1016/j.fuel.2018.07.100.

Krumm, R., Howard, J., 2019. Combined inversion recovery and CPMG NMR interpretation method for more accurate quantification of liquid saturations in organic rich mudstones. In: Unconventional Resources Technology Conference

(URTEC).
Lee, H., Abarghani, A., Liu, B., Shokouhimehr, M., Ostadhassan, M., 2020. Molecular weight variations of kerogen during maturation with MALDI-TOF-MS. Fuel 269, 117452. https://doi.org/10.1016/j.fuel.2020.117452.
Li, J., Huang, W., Lu, S., Wang, M., Chen, G., Tian, W., 2018. Nuclear magnetic resonance T_1 –T_2 map division method for hydrogen-bearing components in continental shale. Energy Fuels 32 (9), 9043–9054.
Li, J., Jiang, C., Wang, M., Lu, S., Chen, Z., et al., 2020. Adsorbed and free hydrocarbons in unconventional shale reservoir: a new insight from NMR T_1-T_2 maps. Mar. Petrol. Geol., 104311 https://doi.org/10.1016/j.marpetgeo.2020.104311.
Liu, K., Ostadhassan, M., Zhou, J., Gentzis, T., Rezaee, R., 2017. Nanoscale pore structure characterization of the Bakken shale in the USA. Fuel 209, 567–578. https://doi.org/10.1016/j.fuel.2017.08.034.
Liu, K., Jin, Z., Zeng, L., Yuan, Y., Ostadhassan, M., 2021. Energy & Fuels 35 (22), 18406–18413.
Liu, B., Bai, L., Chi, Y., Jia, R., Fu, X., Yang, L., 2019. Geochemical characterization and quantitative evaluation of shale oil reservoir by two-dimensional nuclear magnetic resonance and quantitative grain fluorescence on extract: a case study from the Qingshankou Formation in Southern Songliao Basin, northeast China. Mar. Petrol. Geol. 109, 561–573. https://doi.org/10.1016/j.marpetgeo.2019.06.046.
Miao, Y., Zhao, M., Lin, J., Lei, Y., 2017. Application of an improved maximum correlated kurtosis deconvolution method for fault diagnosis of rolling element bearings. Mech. Syst. Signal Process. 92, 173–195. https://doi.org/10.1016/j.ymssp.2017.01.033.
Nicot, B., Vorapalawut, N., Rousseau, B., Madariaga, L.F., Hamon, G., Korb, J.P., 2016. Estimating saturations in organic shales using 2D NMR. Petrophysics 57, 19–29, 01.
Riad, S.M., 1986. The deconvolution problem: an overview. Proc. IEEE 74 (1), 82–85.
Sin, S.K., Chen, C.H., 1992. A comparison of deconvolution techniques for the ultrasonic nondestructive evaluation of materials. IEEE Trans. Image Process. 1 (1), 3–10. https://doi.org/10.1109/83.128026.
Song, Y.Q., Zielinski, L., Ryu, S., 2008. Two-dimensional NMR of diffusion systems. Phys. Rev. Lett. 100 (24), 248002. https://doi.org/10.1103/PhysRevLett.100.248002.
Sorelli, L., Constantinides, G., Ulm, F.J., Toutlemonde, F., 2008. The nano-mechanical signature of ultra-high performance concrete by statistical nanoindentation techniques. Cement Concr. Res. 38 (12), 1447–1456. https://doi.org/10.1016/j.cemconres.2008.09.002.
September Tinni, A., Sondergeld, C., Rai, C., 2014. NMR T_1-T_2 response of moveable and no_n-$m_o$veable fluids in conventional and unconventional rocks. In: Avignon, France (Ed.). International symposium of the society of core analysts, avignon, pp. 8–11.
Tkachenko, A., Van Reeth, T., Tsymbal, V., Aerts, C., Kochukhov, O., Debosscher, J., 2013. Denoising spectroscopic data by means of the improved least-squares deconvolution method. Astron. Astrophys. 560, A37. https://doi.org/10.48550/arXiv.1310.3198.
Ulm, F.J., Vandamme, M., Bobko, C., Alberto Ortega, J., Tai, K., Ortiz, C., 2007. Statistical indentation techniques for hydrated nanocomposites: concrete, bone, and shale. J. Am. Ceram. Soc. 90 (9), 2677–2692. https://doi.org/10.1111/j.1551-2916.2007.02012.x.
Zhong, J., Yan, R., Zhang, H., Feng, Y., Li, N., Liu, X., 2020. A decomposition method of nuclear magnetic resonance T_2 spectrum for identifying fluid properties. Petrol. Explor. Dev., 202088 https://doi.org/10.1016/S1876-3804(20)60089-1.